

Loading of Hip Measured by Hip Contact Forces at Different Speeds of Walking and Running

Georgios Giarmatzis,¹ Ilse Jonkers,² Mariska Wesseling,² Sam Van Rossom,² and Sabine Verschueren¹

¹Research Group for Musculoskeletal Rehabilitation, Department of Rehabilitation Sciences, Katholieke Universiteit Leuven, Heverlee, Belgium

²Human Movement Biomechanics Research Group, Department of Biomedical Kinesiology, Katholieke Universiteit Leuven, Heverlee, Belgium

ABSTRACT

Exercise plays a pivotal role in maximizing peak bone mass in adulthood and maintaining it through aging, by imposing mechanical loading on the bone that can trigger bone mineralization and growth. The optimal type and intensity of exercise that best enhances bone strength remains, however, poorly characterized, partly because the exact peak loading of the bone produced by the diverse types of exercises is not known. By means of integrated motion capture as an input to dynamic simulations, contact forces acting on the hip of 20 young healthy adults were calculated during walking and running at different speeds. During walking, hip contact forces (HCFs) have a two-peak profile whereby the first peak increases from 4.22 body weight (BW) to 5.41 BW and the second from 4.37 BW to 5.74 BW, by increasing speed from 3 to 6 km/h. During running, there is only one peak HCF that increases from 7.49 BW to 10.01 BW, by increasing speed from 6 to 12 km/h. Speed related profiles of peak HCFs and ground reaction forces (GRFs) reveal a different progression of the two peaks during walking. Speed has a stronger impact on peak HCFs rather than on peak GRFs during walking and running, suggesting an increasing influence of muscle activity on peak HCF with increased speed. Moreover, results show that the first peak of HCF during walking can be predicted best by hip adduction moment, and the second peak of HCF by hip extension moment. During running, peak HCF can be best predicted by hip adduction moment. The present study contributes hereby to a better understanding of musculoskeletal loading during walking and running in a wide range of speeds, offering valuable information to clinicians and scientists exploring bone loading as a possible nonpharmacological osteogenic stimulus. © 2015 American Society for Bone and Mineral Research.

KEY WORDS: OSTEOPOROSIS; BIOMECHANICS; EXERCISE; HIP CONTACT FORCES; MUSCULOSKELETAL MODELING

Introduction

As the world population ages, osteoporosis continues to result in an exponential increase in falls and resulting low-trauma fractures, representing increasingly important public health concerns.⁽¹⁾ The costs of osteoporosis related fractures are estimated to increase in the United States to \$25.3 billion yearly by 2025 and in the European Union to a yearly cost of €77 billion by 2050.⁽²⁾ Especially, hip fracture incidence is predicted to increase from 1.66 million in 1990 to 6.26 million in 2050 worldwide and is associated with the largest mortality rates in both genders, compared to the combined risk of the remainder of osteoporotic fractures.⁽³⁾ Therefore, the development of effective strategies to prevent bone loss at the hip constitutes an important and urgent scientific challenge, targeting both maximization of peak bone mass during adulthood⁽⁴⁾ and maintaining it through aging.

Physical activity constitutes an important strategy against osteoporosis, due to the mechanical loading that occurs at the

bone and its beneficial effect on bone mineralization and growth.⁽⁵⁾ For that reason, a large variety and combinations of weight-bearing exercises have been studied in clinical trials to establish activity profiles that have a positive effect on hip bone mineral density (BMD). Results from exercise interventions on postmenopausal women have shown that there can be a significant positive effect of exercise on total hip (area of trochanter and femoral neck) BMD⁽⁶⁾; however, the effect is highly dependent on the type and combination of exercises used. According to a meta-analysis by Martyn-St James and Carroll,⁽⁷⁾ mixed loading protocols that combine jogging with either stair climbing or walking benefit total hip BMD in postmenopausal women, whereas walking alone may have a positive effect on femoral neck BMD.⁽⁸⁾ More interestingly, Borer and colleagues⁽⁹⁾ showed that walking speeds above 6.14 km/h for 4.8 km/day during 4 days a week are effective for bone mineral preservation and growth in postmenopausal women. In addition, high-impact exercises such as running, that load bones with a rapidly rising force profile, improve skeletal integrity in

This article was published online on 22 May 2015. An error was subsequently identified. This notice is included in both the online and print versions to indicate that both have been corrected on 4 July 2015.

Received in original form December 18, 2014; revised form February 12, 2015; accepted February 17, 2015. Accepted manuscript online February 19, 2015.

Address correspondence to: Sabine Verschueren, PhD, Research Group for Musculoskeletal Rehabilitation, Department of Rehabilitation Sciences, Katholieke Universiteit Leuven, Tervuursevest 101, B-3001 Heverlee, Belgium. E-mail: sabine.verschueren@faber.kuleuven.be

Additional Supporting Information may be found in the online version of this article.

Journal of Bone and Mineral Research, Vol. 30, No. 8, August 2015, pp 1431–1440

DOI: 10.1002/jbmr.2483

© 2015 American Society for Bone and Mineral Research

premenopausal women and may potentially reduce the risk of osteoporosis in later life.^(10,11) Nevertheless, the optimal type, intensity, frequency and duration of exercises that enhance bone mass are still largely unknown, due to the knowledge gap on how different loading paradigms best protect cortical and/or trabecular bone density and strength. Carefully designed biomechanical studies describing joint impact in terms of peak joint contact forces at different intensities of a single exercise can help inform that gap.

To allow prediction of the osteogenic effect of different exercise programs on the hip, quantitative data are needed on calculated forces acting on the hip joint. These forces produce stresses and strains in the femoral neck that are responsible for either degeneration, preservation, or regeneration of the local bone microstructure.⁽¹²⁾ The potential to relate hip contact forces (HCFs) during different exercises to stresses and strain levels known to trigger osteogenesis could be a major advancement toward optimizing training programs that induce appropriate force levels to stimulate bone formation. Direct measurement of HCFs is only feasible in subjects who have received instrumented implant, allowing the recording of signals from strain gauges integrated in the implant.^(13,14) Although these measurements are considered as the "gold standard" for hip loadings, limitations such as altered anatomy and physiology of the hip region due to surgery, the small number and old age of the subjects, and the altered gait characteristics of the hip implanted patients,⁽¹⁵⁾ inhibit clinicians from using these data for designing exercise programs for other populations. However, in vivo measurements remain the only direct source of HCFs.

In a noninvasive way, musculoskeletal models in combination with static optimization techniques have been used to calculate muscle forces and hence joint loading during movement. These techniques use experimental kinematics and kinetics as inputs. Musculoskeletal modeling has been successfully used in numerous studies focusing on musculoskeletal loading during gait. Several studies showed that HCFs in total hip arthroplasty (THA) patients predicted by musculoskeletal models during walking are comparable to experimental values,^(16–18) showing the strength of simulation techniques and allowing scientists to extend their research on healthy subjects too.

The present study focuses on walking and running as two of the most common exercises used in recreational sports and rehabilitation programs. Based on previously reported increase in GRFs,⁽¹⁹⁾ kinetics and muscle activations^(20,21) with walking speed and running,⁽²²⁾ we hypothesize that HCFs will increase with increasing speed as well. Several simulation studies have calculated HCFs during walking^(16,17,23,24) and running.^(23,25,26) However, the relationship between peak HCFs and speed is less described during walking^(27,28) and has not been assessed for running. Discrepancies in optimization techniques and the use of different musculoskeletal models also necessitate a critical review of these studies. At the same time, extending the existing knowledge on speed effect of HCFs to running is required.

Today, knowledge on optimal exercise parameters that can effectively trigger osteogenesis at the hip combined with feasibility and safety for elderly populations is still lacking. Although numerous clinical trials with exercise have been carried out, large discrepancies among them do not allow scientists to safely choose effective exercise interventions. Calculation of joint forces through modeling, and—as a second step in the future—stresses/strains through finite element analysis,^(29,30) will offer a fundamental insight into bone reaction

to external loadings and reveal which exercises and intensities can potentially be effective to produce an osteogenic effect at the hip bone site. The current study aims to offer a fundamental insight into musculoskeletal loading during walking and running and, more specifically, to evaluate the effect of speed, hence contributing to the design of future safer and more effective exercise interventions.

Materials and Methods

Participants

Twenty young healthy participants, 10 female and 10 male (mean \pm SD; age 22.2 ± 1.6 years; height: 1.75 ± 0.09 m; weight: 65.7 ± 7.8 kg; BMI: 21.5 ± 1.7 kg/m²) volunteered for this study. The study was approved by the local Ethics Committee and informed consent was obtained from all subjects. Volunteers were recruited among university students. Exclusion criteria were prior conditions that might affect their performance, such as pain, lower limb fracture, and surgery.

Gait analysis

Subjects were instructed to walk and run barefoot on a motor-driven treadmill (Forcelink, Culemborg, The Netherlands) at speeds ranging between 3 and 12 km/h, with an increment of 1 km/h. Selection of the speed range was based upon the rationale of commonly used speeds used in exercise interventions and rehabilitation programs. For subjects' safety, a harness attached to the ceiling was used to hold their body, in case of treadmill failure or fall.

Subjects were instructed to independently choose their transition speed from walking to running, look forward, and move their hands freely. They chose a different speed to transition from walking to running: 7 subjects chose to run at 6 km/h, and 13 subjects at 7 km/h. One subject was not able to run above 9 km/h, due to uneasiness. Because counting steps during walking and especially running was practically difficult, data collection was done for 10 s following an adaptation period of 10 s. Because all subjects had previous experience in walking/running on a treadmill, data collection was completed within 4 minutes, except for the subject that did not finish the protocol.

Fifty retroreflective markers (Fig. 1) were placed on the participants' bodies and their 3D trajectories were captured using a 10-camera VICON system (10-15 MX camera system; Vicon, Oxford Metrics, Oxford, UK) sampling at 100 Hz. Clustered markers were placed on the thigh and tibia for better tracking of these body segments. Medial markers at the knee and ankle joint were removed during dynamic trials in order to avoid adaptation of natural movement in case of marker contact. GRFs and torques were measured by two force plates integrated in the treadmill sampling at 1000 Hz.

Musculoskeletal modeling

To process the kinematic data, the following steps in OpenSim (Stanford University, CA, USA)⁽³¹⁾ were followed (Fig. 2):

1. A generic musculoskeletal model with 23 degrees of freedom (DOF) and 92 Hill-type muscle-tendon actuators⁽³²⁾ was scaled to match the anthropometry of each subject using the marker positions recorded during a static trial. The hip joint was modeled as a ball-in-socket 3-DOF joint,

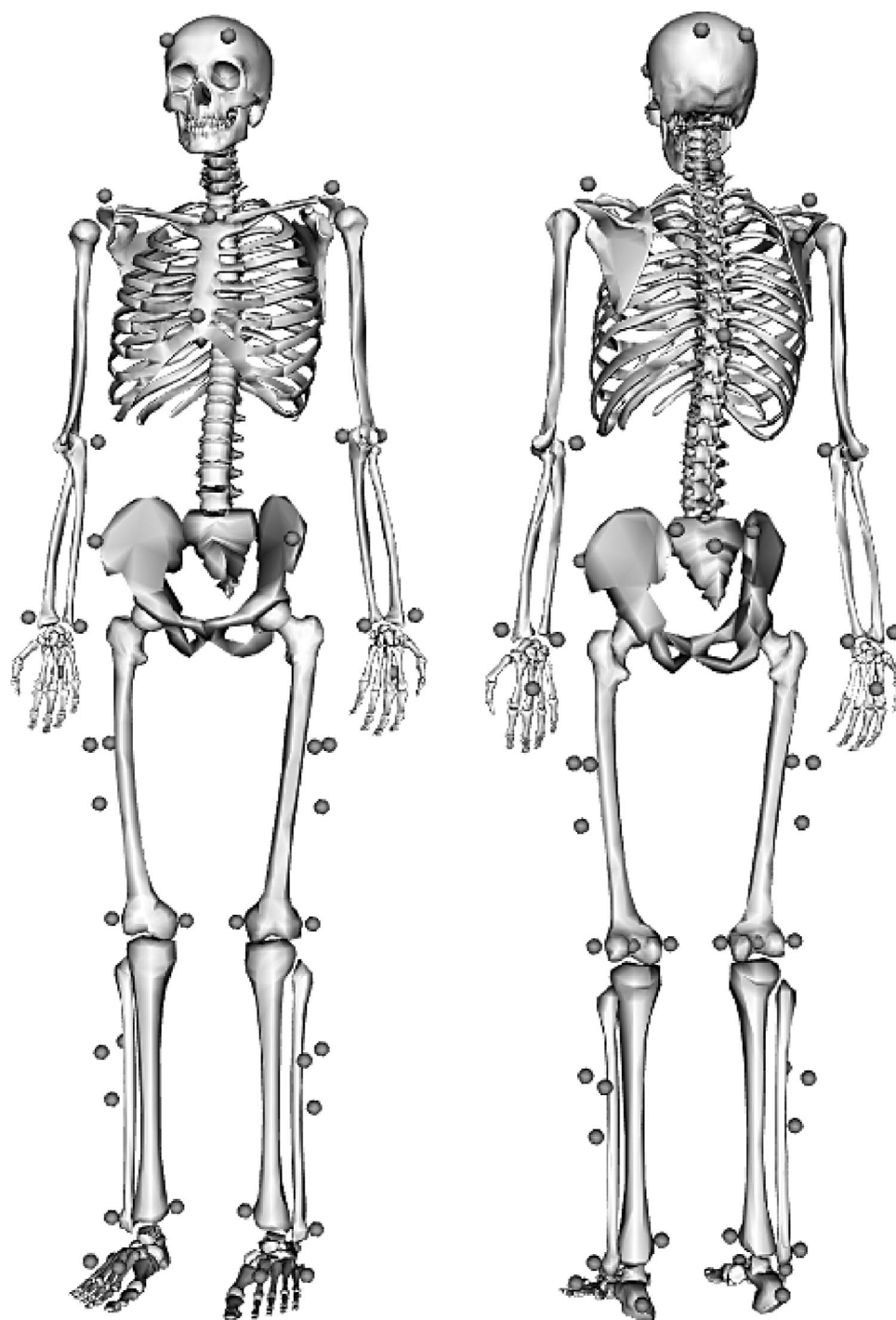


Fig. 1. Marker set used for motion capture.

whereas for the knee and ankle a 1-DOF joint was implemented.⁽³³⁾ Subtalar and metatarsophalangeal joints were locked in neutral anatomical angles.

2. After labeling the markers in Nexus software (version 1.8.2; Vicon), a Kalman smoothing algorithm was used to calculate the joint angles during movement using the marker trajectories and based on the musculoskeletal model definition.⁽³⁴⁾

3. Using the kinematics from the previous step and measured GRFs as an input, the joint moments were calculated using an inverse dynamics analysis implemented in Opensim. A low-pass filter with a cutoff of 6 Hz was used on kinematics and GRFs.
4. Thereafter, a muscle force distribution problem was solved using the static optimization algorithm in OpenSim. The algorithm estimates muscle activations and forces during a

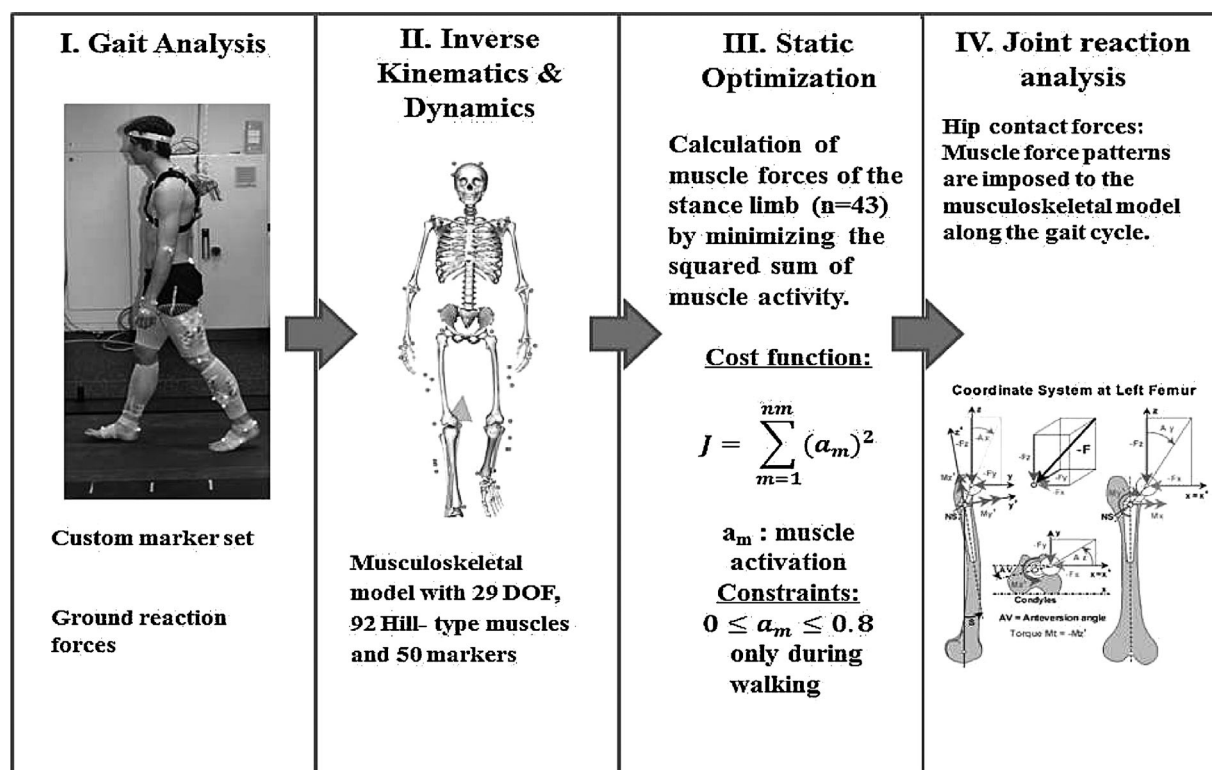


Fig. 2. Workflow used for calculation of HCFs. A generic model of 12 segments and 29 degrees of freedom was used in the analysis. HCF = hip contact force; DOF = degree of freedom.

specific motion, by distributing the intersegmental joint moments to the muscles involved in equilibrating them.⁽³⁵⁾ The cost function was set to minimize the squared sum of all muscle activations. Because symmetry in walking and running moving patterns can be assumed,⁽³⁶⁾ only the muscle forces of 43 muscles of the right leg in the model were estimated. Reserve actuators were added to the joints of the model and to the pelvis-ground joint, to provide the additional torques if needed during static optimization. High reserve actuators around the hip in the frontal plane were observed in some subjects during high-speed movements. Therefore, a specific workflow was implemented to account for the contribution of the reserve actuator torque that was provided at the joints in the calculation of hip contact forces. In a postanalysis step, the torque generated by the hip abduction reserve actuator was distributed along the three bundles of the gluteus medius according to the percent contribution of each individual bundle to the total force of the summed bundles. By accounting for the instantaneous moment arm of the bundles, the percent torque contribution was converted to an additional force component that was added to the force production of the individual muscle bundles calculated following the static optimization step.

5. Using the joint reaction analysis in Opensim, the three components of HCF and the resultant HCF were calculated in the femur coordinate system.

Resultant HCFs and vertical GRFs were normalized to subjects' body weight (BW) (divided by body weight in Newtons) and moments to subjects' body mass (Nm/kg).⁽³⁷⁾

Statistics

Individual gait cycles were identified and all data was time normalized to 100 points by spline interpolation. A first averaging process resulted in an ensemble average curve for each subject at every speed. These curves were then used for the second averaging process between subjects, resulting in ensemble curves of GRFs and HCFs and hip moments along the three planes for every speed. A similar process was followed for mean peak values. First, peak values were identified in every gait cycle of every speed and a first averaging process resulted in mean peak values for every subject (Fig. 3). A second averaging process between subjects resulted in the mean peak values for every speed (Tables 1, 2). Percentage increase (PI) of mean peak magnitudes between extreme speeds during walking and running were calculated as an indicator of change with speed.

Because of missing data at the speed of 6 km/h given the different transition speed for each subject, linear mixed-effect analysis was chosen as it can handle unbalanced data sets and take into account individual trends for regression analysis. The linear mixed model was applied using SPSS 19.0 (IBM SPSS Statistics for Windows, Armonk, NY, USA). Our model consisted of two parts; speed was used as a fixed effect and intercept and slope for each subject were used as random effects, in order to account for subject variability. In order to determine which type of relationship best described the relation between each dependent variable and speed (linear or quadratic), squared speed was additionally included as a fixed effect and its effect on the level of significance was tested.⁽³⁸⁾ Regression lines were defined based on the predicted values of HCFs and GRFs, which

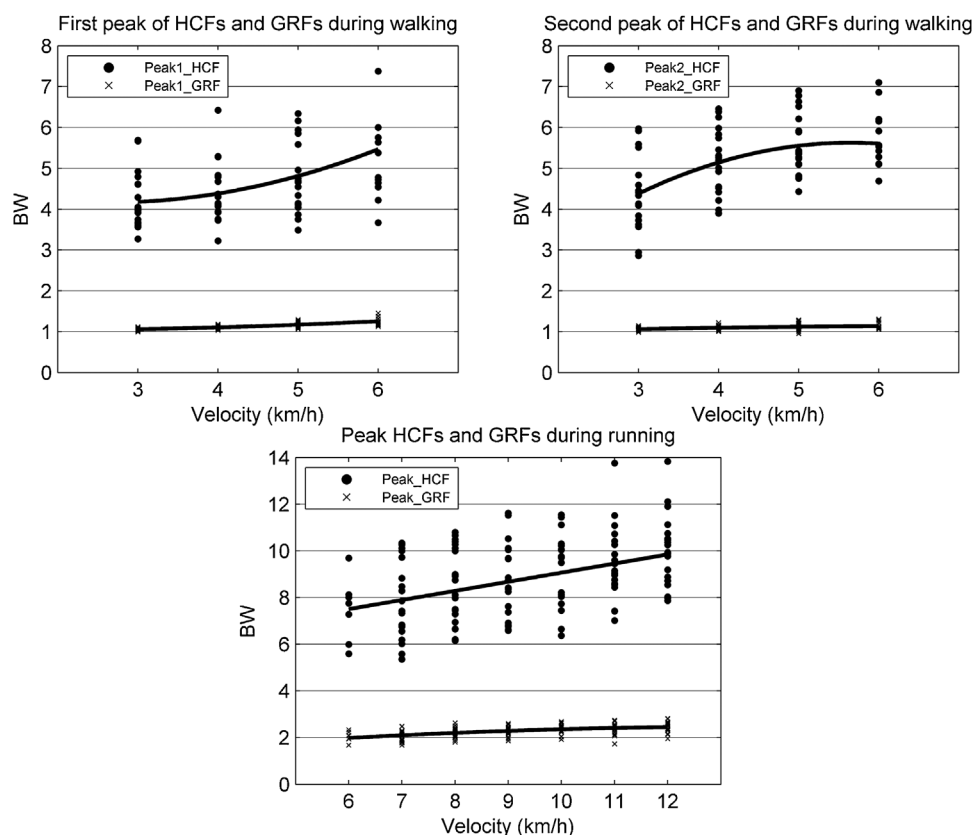


Fig. 3. Distribution of peak GRFs and peak HCFs at different speeds during walking and running. GRF = ground reaction force; HCF = hip contact force.

our analysis produced for every speed. Peak magnitudes were analyzed for significant speed effect. Descriptive statistics and comparisons between parameters at different speeds were performed when speed was considered as a categorical variable. For multiple comparisons, a Bonferroni correction was applied. All significance levels were set to 0.05.

Results

Ensemble GRF and HCF curves for both walking and running are shown in Figs. 4, 5, respectively. Positive HCFs indicate downward and positive GRFs indicate upward direction. Pairwise comparisons between speeds for peak GRFs, HCFs during walking and running are summarized in Tables 1 and 2.

The ensemble curves of hip flexion/extension, hip abduction/adduction and hip internal/external rotation moments (Supporting Fig. 1), as well as the three components of HCFs (Supporting Fig. 2) during walking and running at different speeds are provided as supplementary material.

During walking, vertical GRFs as well as resultant HCFs, have a two-peak profile, one peak during initial double support (first 0% to 30% of the gait cycle) and one peak during terminal double support (40% to 60% of the gait cycle) (Figs. 4, 5). Speed had a significant effect on all peak GRFs (Tables 1, 2). Mean values increase from 1.06 BW to 1.24 BW for the first peak (Peak1_GRF) and 1.06 BW to 1.14 BW for the second (Peak2_GRF) (Table 1). During running, there is only one peak during stance phase (Peak_GRF), which also increases with speed from a mean value of 2.05 BW to a value of 2.47 BW (Table 2). Distribution of

Table 1. Peak GRFs and HCFs During Walking

Velocity	3 km/h	4 km/h	5 km/h	6 km/h	Speed effect (<i>p</i>)
Peak1_GRF (BW)	1.06 ± 0.03 ^{a,b,c}	1.10 ± 0.05 ^{b,c}	1.17 ± 0.06 ^c	1.25 ± 0.10	<0.001
Peak2_GRF (BW)	1.06 ± 0.04 ^{a,b,c}	1.09 ± 0.06 ^{b,c}	1.12 ± 0.09 ^c	1.14 ± 0.08	<0.001
Peak1_HCF (BW)	4.22 ± 0.70 ^{b,c}	4.39 ± 0.72 ^{b,c}	4.80 ± 0.90 ^c	5.41 ± 1.31	<0.001
Peak2_HCF (BW)	4.37 ± 0.92 ^{a,b,c}	5.15 ± 0.81 ^{b,c}	5.54 ± 0.76 ^c	5.74 ± 0.73	<0.001

Values are mean ± SD. Significance level of pairwise comparisons and speed effect is *p* < 0.05.

GRF = ground reaction force; HCF = hip contact force; Peak1 = first peak; BW = body weight; Peak2 = second peak.

^aSignificantly different from 4 km/h.

^bSignificantly different from 5 km/h.

^cSignificantly different from 6 km/h.

Table 2. Peak GRFs and HCFs During Running

Velocity	6 km/h	7 km/h	8 km/h	9 km/h	10 km/h	11 km/h	12 km/h	Speed (<i>p</i>)
Peak_GRF (BW)	2.05 ± 0.22 ^{a,b,c,d,e}	2.08 ± 0.22 ^{a,b,c,d,e}	2.22 ± 0.21 ^{b,c,d,e}	2.30 ± 0.19 ^e	2.37 ± 0.20 ^e	2.38 ± 0.25 ^e	2.47 ± 0.23	<0.001
Peak_HCF (BW)	7.49 ± 1.38 ^{c,d,e}	7.77 ± 1.64 ^{a,b,c,d,e}	8.52 ± 1.62 ^{d,e}	8.56 ± 1.65 ^{d,e}	9.12 ± 1.66 ^e	9.47 ± 1.62	10.01 ± 1.55	<0.001

Values are mean ± SD. Significance level of pairwise comparisons and speed effect is $p < 0.05$.
GRF = ground reaction force; HCF = hip contact force; Peak = peak during running; BW = body weight.
^aSignificantly different from 8 km/h.
^bSignificantly different from 9 km/h.
^cSignificantly different from 10 km/h.
^dSignificantly different from 11 km/h.
^eSignificantly different from 12 km/h.

peak GRFs during walking and running are shown in Fig. 3. The analysis showed that Peak1_GRF increases quadratically ($F(1, 50.14) = 5.07, p = 0.029$) with a PI of 17%, with higher increase rates at higher speeds, whereas Peak2_GRF increases linearly ($F(1, 53.83) = 29.05, p < 0.001$) with a PI of 8%. For running, Peak_GRF increases quadratically ($F(1, 73.58) = 16.91, p < 0.001$) with a PI of 21%, with lower rates of increase at higher speeds.

Ensemble curves of the resultant HCFs in four walking speeds and seven running speeds are shown in Fig. 5. Speed had a significant effect on all peak HCFs (Tables 1, 2). Mean values increase from 4.22 BW to 5.41 BW for the first peak (Peak1_HCF) and 4.37 BW to 5.74 BW for the second peak (Peak2_HCF) (Table 1). During running, one peak occurs along the stance phase at 0% to 30% of the gait cycle (Peak_HCF) and it increases with speed from 7.49 BW to 10.01 BW (Table 2). A second much smaller peak occurs during swing phase and is highly variable from subject to subject. Distribution of peak HCFs and regression lines are shown in Fig. 3. Our analysis showed a significant quadratic increase for Peak1_HCF ($F(1, 42.22) = 5.21, p = 0.028$) with a PI of 28%, with higher increase rates at higher

speeds, and for Peak2_HCF ($F(1, 33.25) = 16.15, p < 0.001$) with a PI of 31%, with lower increase rates at higher speeds. For running, a significant linear increase with speed was found ($F(1, 25.36) = 104.11, p < 0.001$) with a PI of 34%.

In order to identify the best predictors of peak HCFs among the clinically easier to calculate hip moments, coefficient of determination (R^2) values from linear regression analysis between peak HCFs and coincided hip moments from the ensemble average curves were obtained for each speed (Tables 3, 4). Results for running at 6 km/h were not obtained because of insufficient data. According to our analysis, hip adduction moment best predicts Peak1_HCF in walking with an average R^2 value of 0.60 (range, 0.53 to 0.78) and Peak_HCF in running with an average R^2 value of 0.69 (range, 0.63 to 0.72), whereas hip extension moment best predicts Peak2_HCF in walking with an average R^2 value of 0.58 (range, 0.63 to 0.89). In some cases, combinations of moments in a multiple regression model were also found to increase the R^2 value significantly (Tables, 4 3). During walking, hip flexion and external rotation combined better predicted Peak1_HCF at 3 km/h, hip adduction and hip extension moment combined

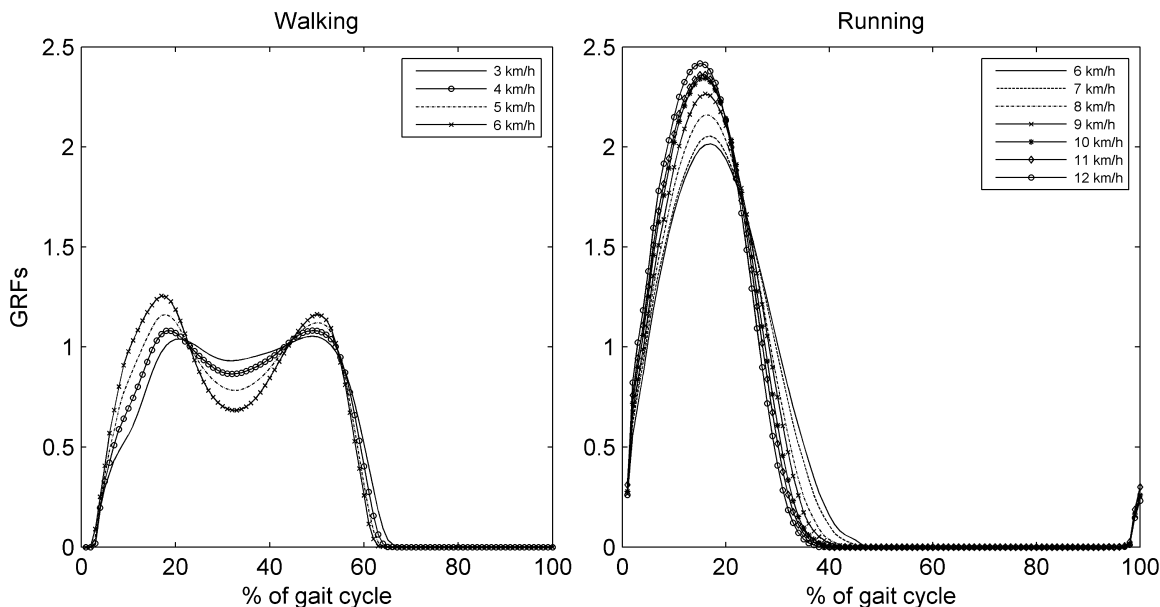


Fig. 4. Ensemble curves of GRFs in different speeds during walking and running along the gait cycle. GRF = ground reaction force.

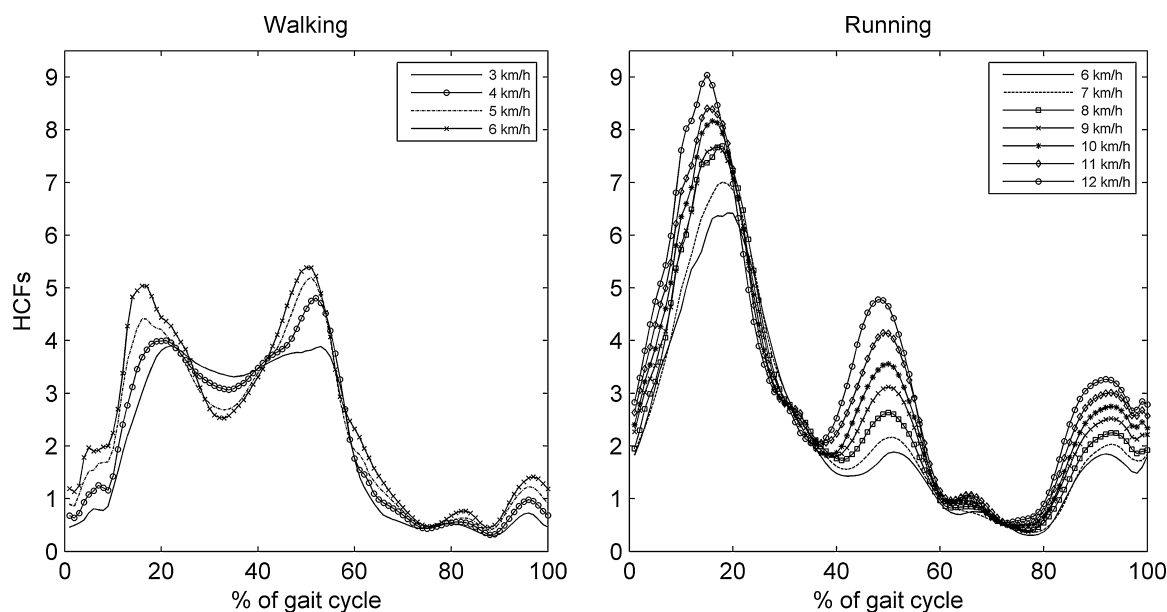


Fig. 5. Ensemble curves of HCFs in different speeds during walking and running along the gait cycle. HCF = hip contact force.

better predicted Peak1_HCF at 6 km/h. During running, hip adduction combined with external rotation moment better predicted Peak_HCF at 8 and 10 km/h. However, over all speeds no firm conclusions can be drawn to put a combination of moments forward for HCF prediction for either walking or running.

Discussion

This study analyzed the effect of velocity during walking and running on peak GRFs and HCFs through motion analysis and musculoskeletal modeling. Although exercise interventions primarily target middle-aged and elderly populations, information about musculoskeletal loading during exercise in young populations is important for designing "osteogenic" training programs, because peak bone mass acquired during adulthood is a crucial determinant of bone strength in later life. So research on biomechanics of exercise in young can help inform later the development of adjusted training programs for elderly. Additionally, we choose to measure young healthy subjects

first, as they can perform a wider range of speeds of the movements tested. Future work will assess HCFs during walking and running in elderly subjects at adjusted speeds. Ensemble curves of moments around the hip, the GRF and the HCF magnitude were also estimated at different speeds.

Knowledge of reference values of peak HCFs in different speeds during walking and running, along with the nature of that relationship, is of utter importance for scientists looking at the dynamic loading of the musculoskeletal system and its implications. Our findings are comparable to former studies. Values between 4.22 BW and 5.41 BW for Peak1_HCF and between 4.37 BW and 5.74 BW for Peak2_HCF calculated in this study compare favorably with 2.9 BW to 5.7 BW⁽²⁸⁾ and 3 BW to 6.5 BW⁽²⁷⁾ predicted previously. In vivo peak values of HCFs from THA patients⁽¹⁴⁾ in walking speeds of 3 and 5 km/h also compare favorably to our values in the same speeds, serving as a validation to our findings. In the same study, in vivo values around 5 BW during running were found at 7 and 8 km/h, which is much lower than ours but still higher than during walking (~3 BW). Nevertheless, direct comparison between young adults and elderly THA patients during running should be made with

Table 3. R^2 Values From Regression Analysis Between Peak HCFs and the Three Hip Moments as Predictors During Walking

Predictor	3 km/h		4 km/h		5 km/h		6 km/h	
	Peak1	Peak2	Peak1	Peak2	Peak1	Peak2	Peak1	Peak2
Hip adduction moment	0.53*	0.16	0.53*	0.17	0.54*	0.09	0.78*	0.12
Hip extension moment	0.001	0.52*	0.04	0.51*	0.14	0.61*	0.17	0.7*
Hip internal/external rotation moment	0.04	0.44*	0.02	0.03	0.07	0.01	0.02	0.12
Hip flexion + hip external rotation		0.66*						
Hip adduction + hip extension							0.93*	

Values with (*) were found to be significant when $p < 0.05$. Stepwise regression was used to examine if the R^2 value changes significantly when a second predictor is added; such significant changes are also shown.

HCF = hip contact force; Peak1 = first peak; Peak2 = second peak.

Table 4. R^2 Values From Regression Analysis Between Peak HCFs and the Three Hip Moments as Predictors During Running

Predictor	7 km/h	8 km/h	9 km/h	10 km/h	11 km/h	12 km/h
Hip adduction moment	0.71*	0.68*	0.73*	0.63*	0.68*	0.72*
Hip flexion moment	0.002	0.003	0.007	0.0003	0.02	0.006
Hip external rotation moment	0.22	0.6*	0.33*	0.35*	0.32	0.3
Hip adduction + hip rotation		0.81*		0.77*		

Values with (*) were found to be significant at $p < 0.05$. Stepwise regression was used to examine if the R^2 value changes significantly when a second predictor is added. Such significant changes are also shown.

HCF = hip contact force.

caution, because of the different performance between the two age groups in such dynamic conditions.⁽³⁹⁾ Previous simulation studies have calculated peak HCFs during running in young healthy subjects reporting 7.9 BW at 15.3 km/h,⁽²⁶⁾ 11.9 BW at 15.8 km/h.⁽²⁵⁾ In the study of van den Bogert et al.⁽²³⁾ accelerometry in combination with modeling has been used and rather low HCF values of 5.2 BW at 12.6 km/h were found, however this large deviation from the aforementioned results is most likely related to the assumptions and methodology applied in this study. Our results show that peak HCFs during running are higher than in walking and range from 7.49 BW to 10.01 BW in a speed range of 6 to 12 km/h. When assessing the changes in HCF by increasing the speed, our study reports a quadratic increase in peak HCFs during walking but linear increase during running (Fig. 3). During walking, Röhrle and colleagues⁽²⁸⁾ found that both peaks of HCF increase linearly with speed, whereas Crowinshield and colleagues⁽²⁷⁾—although not discriminating between the two peaks—showed a quadratic increase of peak values in the young group, with higher increase rate in higher speeds, and a linear increase for the old group. Differences in motion capturing protocol and modeling techniques are potential reasons for discrepancies between those findings and ours. Our results show a different pattern of increase with speed for both peaks of HCFs during walking, with the first one (Peak1_HCF) increasing faster at higher speeds than the second one (Peak2_HCF). According to Pandy and Andriacchi,⁽⁴⁰⁾ the underlying reason for that difference is that the muscles mainly responsible for the hip loading (gluteus medius, gluteus maximus, iliopsoas, rectus femoris, and hamstrings) have different activation patterns at the two phases, and thus apply different forces onto the hip. According to the same authors,⁽⁴⁰⁾ the first peak of HCF is mainly attributed to gluteus medius, gluteus maximus, and rectus femoris activation, whereas the second peak of HCF later in the stance phase to gluteus medius, iliopsoas, and rectus femoris activation. Overall, this difference is related to the different kinetics during these phases in the gait cycle and to separate musculoskeletal demands. Results from the regression analysis (Table 3) further clarify this discrepancy in the contributors to the HCF, indicating hip adduction moment as a better predictor for Peak1_HCF and hip extension moment for Peak2_HCF. This finding demonstrates the fact that different muscle groups are dominantly activated during the two peaks in walking: hip abductors for the first peak and hip flexors for the second. During running, hip adduction best predicts peak HCFs in all speeds, relating again the hip abductors' function with peak hip joint loading. These insights could be used in future research to specifically target key muscle groups for strengthening by opting for either walking or running. Furthermore, this opens some perspectives for therapy and training because nowadays real-time feedback

systems that can provide real-time information on joint moments⁽⁴¹⁾ are beginning to be integrated into clinical 3D motion capture systems. These joint moments can then be used as surrogate marker representative for hip joint loading and provide feedback on gait strategies aiming to further load or unload the hip joint accordingly.

It is obvious that walking and running impose a different muscular demand on the musculoskeletal system. In our study subjects chose either to walk or run at 6 km/h. According to our results, walking at that speed corresponds to mean peak HCFs of 5.41 BW (Peak1_HCF) and 5.74 BW (Peak2_HCF). Conversely, during running at the same speed, or "jogging," HCFs are much larger, with a mean of 7.49 BW. Apparently, although jogging at 6 km/h can be presumed as a mild exercise, the large differences in peak HCFs seen between walking and running at this speed need to be taken into account. This knowledge can be crucial to practitioners who design programs that include either walking or running.

Based on the regression lines of GRFs and HCFs in function of speed (Fig. 3) and the apparent magnitude difference, it needs to be concluded that GRFs are possibly not good predictors of peak skeletal loading at the hip. Therefore the use of GRFs to determine whether an exercise would exceed an osteogenic threshold, as done in previous studies,⁽⁹⁾ can be misleading. Röhrle and colleagues⁽²⁸⁾ interestingly already argued that GRFs might be "insufficient to interpret joint forces," because of their small variability (~7%) in contrast to the large variability (20% to 25%) of HCFs they calculated in their study. Our findings support that argument in several ways. First, we confirmed that small intersubject variability in peak GRFs does not seem to account for the large intersubject variability seen in peak HCFs. GRFs' variability for walking was found to be ~3% to 8% and ~8% to 10% for running, whereas HCFs' variability was ~13% to 25% and ~16% to 20%, respectively. Second, the percent increase of peak HCFs in walking (28% for Peak1_HCF and 31% for Peak2_HCF) and running (34%) are larger than in the case of peak GRFs in walking (17% for Peak1_GRF and 8% for Peak2_GRF) and running (21%). Therefore, the magnitude of peak HCFs increases more rapidly with increasing speed than that of GRFs. As a consequence, GRF data may not be appropriate to discriminate skeletal loading between velocity increments as they only present limited increase. To conclude, discrepancies between HCFs and GRFs discussed here suggest that other factors, such as muscle activity, do play an important role to the hip loading. This is related to the fact that muscles crossing the hip joint exert considerable forces to equilibrate the external moments caused by GRFs around this joint during a given motion. Therefore, although trainers usually tend to rely on GRFs to assess the intensity of an exercise regimen, this study shows that knowledge of hip joint forces is imperative to acquire

a deeper insight into the bone loading during a particular exercise at a given speed and to safely choose the appropriate training intensity.

The goal of our study was to calculate HCFs during different speeds in walking and running, and investigate the relationship between peak values and velocity. However, our results should be used and interpreted with caution, because of the inherent limitations related to subject sample, protocol, and simulation process. Peak hip loading from young adults cannot be generalized to elderly populations, given the differences in motion strategy during walking⁽⁴²⁾ and running⁽³⁹⁾ between these two age groups, more specifically because reduced stride length observed in elderly subjects may result in reduced peak HCFs.⁽²⁴⁾ A follow-up study will address this issue. Moreover, having the subjects walk and run barefoot was chosen in this study to accomplish direct application of GRFs to the foot and a better motion tracking of this segment; however, it has been shown to result in reduced hip joint kinetics compared to the shod condition.^(43,44) Although this theoretically would induce smaller peak HCFs, this effect is yet to be confirmed. Consequently, our results may not apply to all walking and running conditions. Finally, muscle representation in the model inherently is a simplified representation of the actual muscle action in the human body. The simplified muscle models used here may therefore affect the calculation of muscle forces and HCFs—especially in strenuous activities such as running. Moreover, the function of reserve actuators constitutes a confounding factor in the muscle work, because they are activated when muscles cannot produce the necessary force to follow the kinematics. In our study, considerable activation of reserve actuators around hip was noticed mainly at 11 and 12 km/h. However, given the described workflow we accounted for them, under the assumption that all three parts of the gluteus medius included in the model will proportionally account for the moment generated by the reserve actuators. Of course, refinement of musculoskeletal models remains imperative in order to facilitate scientists in simulating especially highly dynamic movements with the minimum “external help,” as now provided by the reserve actuators. Future studies should focus on improving muscle representation and provide more refined musculoskeletal models.

The current study mainly contributes to a better insight on differences in musculoskeletal loading between walking and running and the effect of speed. Changes in peak HCFs and GRFs during walking and running were introduced, providing a more detailed presentation on the relation of both forces with velocity, in a wide range of commonly used speeds. Through modeling, a deeper insight into joint forces was established, illustrating that ground reaction forces and external moments can only partially describe the true musculoskeletal bone loading and that muscle action used to balance external joint moments is an important additional factor in affecting bone loading during different exercises. In future research these results can be used in more elaborate techniques, such as finite element analysis, in order to fully understand the mechanisms underlying bone reaction to load. These analyses, providing stresses and strains at specific target points in particular exercise conditions, can then result in safer and more effective exercise interventions to safeguard individual skeletal load bearing capacity while inducing sufficient training stimuli.

Disclosures

All authors state that they have no conflicts of interest.

Acknowledgments

This work was supported by the Fund for Scientific Research (FWO-Vlaanderen) (G0526512 to SV). We thank all the participants in this study for their outstanding cooperation, as well as Annouschka Laenen from Leuven Biostatistics and Statistical Bioinformatics Centre for her precious help with statistics.

Authors' roles: Study design: GG, SV, and IJ. Study conduct: GG. Data collection: GG and SR. Data analysis: GG, IJ, SV, and MW. Data interpretation: GG, IJ, MW, and SV. Drafting manuscript: GG. Revising manuscript content: IJ and SV. Approving final version of manuscript: IJ, MW, SR, and SV. GG takes responsibility for the integrity of the data analysis.

References

1. Reginster JY, Burlet N. Osteoporosis: a still increasing prevalence. *Bone*. 2006 Feb;38(2 Suppl 1):S4–9.
2. Kuehn BM. Better osteoporosis management a priority: impact predicted to soar with aging population. *JAMA*. 2005 May 25;293(20):2453–8.
3. Boonen S, Dejaeger E, Vanderschueren D, et al. Osteoporosis and osteoporotic fracture occurrence and prevention in the elderly: a geriatric perspective. *Best Pract Res Clin Endocrinol Metab*. 2008 Oct;22(5):765–85.
4. Heaney RP, Abrams S, Dawson-Hughes B, et al. Peak bone mass. *Osteoporos Int*. 2000;11(12):985–1009.
5. Borer KT. Physical activity in the prevention and amelioration of osteoporosis in women: interaction of mechanical, hormonal and dietary factors. *Sports Med*. 2005 Jan;35(9):779–830.
6. Howe TE, Shea B, Dawson LJ, et al. Exercise for preventing and treating osteoporosis in postmenopausal women [Review]. *Cochrane Database Syst Rev*. 2011 Jul 6;(7):CD000333. DOI: 10.1002/14651858.CD000333.pub2 .
7. Martyn-St James M, Carroll S. A meta-analysis of impact exercise on postmenopausal bone loss: the case for mixed loading exercise programmes. *Br J Sports Med*. 2009 Dec;43(12):898–908.
8. Martyn-St James M, Carroll S. Meta-analysis of walking for preservation of bone mineral density in postmenopausal women. *Bone*. 2008 Sep;43(3):521–31.
9. Borer KT, Fogleman K, Gross M, La New JM, Dengel D. Walking intensity for postmenopausal bone mineral preservation and accrual. *Bone*. 2007 Oct;41(4):713–21.
10. Heinonen A, Kannus P, Sievänen H, et al. Randomised controlled trial of effect of high-impact exercise on selected risk factors for osteoporotic fractures. *Lancet*. 1996 Nov 16;348(9038):1343–7.
11. Vainionpää A, Korpelainen R, Leppäluoto J, Jämsä T. Effects of high-impact exercise on bone mineral density: a randomized controlled trial in premenopausal women. *Osteoporos Int*. 2005 Feb;16(2):191–7.
12. Frost HM. Bone's mechanostat: a 2003 update. *Anat Rec A Discov Mol Cell Evol Biol*. 2003;275(2):1081–101.
13. Bergmann G, Deuretzbacher G, Heller M, et al. Hip contact forces and gait patterns from routine activities. *J Biomech*. 2001 Jul;34(7):859–71.
14. Bergmann G, Graichen F, Rohlmann A. Hip joint loading during walking and running, measured in two patients. *J Biomech*. 1993;26(8):969–90.
15. Ewen AM, Stewart S, St Clair Gibson A, Kashyap SN, Caplan N. Post-operative gait analysis in total hip replacement patients—a review of current literature and meta-analysis. *Gait Posture*. 2012 May;36(1):1–6.
16. Heller MO, Bergmann G, Deuretzbacher G, et al. Musculo-skeletal loading conditions at the hip during walking and stair climbing. *J Biomech*. 2001 Jul;34(7):883–93.

17. Stansfield BW, Nicol AC, Paul JP, Kelly IG, Graichen F, Bergmann G. Direct comparison of calculated hip joint contact forces with those measured using instrumented implants. An evaluation of a three-dimensional mathematical model of the lower limb. *J Biomech*. 2003 Jul;36(7):929–36.
18. Lenaerts G, Mulier M, Spaepen A, Van der Perre G, Jonkers I. Aberrant pelvis and hip kinematics impair hip loading before and after total hip replacement. *Gait Posture*. 2009 Oct;30(3):296–302.
19. Keller TS, Weisberger AM, Ray JL, Hasan SS, Shiavi RG, Spengler DM. *Clin Biomech (Bristol, Avon)*. 1996 Jul;11(5):253–9.
20. Cappellini G, Ivanenko YP, Poppele RE, Lacquaniti F. Motor patterns in human walking and running. *J Neurophysiol*. 2006 Jun;95(6):3426–37.
21. Chumanov ES, Wille CM, Michalski MP, Heiderscheit BC. Changes in muscle activation patterns when running step rate is increased. *Gait Posture*. 2012 Jun;36(2):231–5.
22. Schache AG, Blanch PD, Dorn TW, Brown NA, Rosemond D, Pandy MG. Effect of running speed on lower limb joint kinetics. *Med Sci Sports Exerc*. 2011 Jul;43(7):1260–71.
23. van den Bogert AJ, Read L, Nigg BM. An analysis of hip joint loading during walking, running, and skiing. *Med Sci Sports Exerc*. 1999;31 (January 1999):131–42.
24. Stansfield BW, Nicol AC. Hip joint contact forces in normal subjects and subjects with total hip prostheses: walking and stair and ramp negotiation. *Clin Biomech (Bristol, Avon)*. 2002 Feb;17(2):130–9.
25. Edwards WB, Gillette JC, Thomas JM, Derrick TR. Internal femoral forces and moments during running: implications for stress fracture development. *Clin Biomech (Bristol, Avon)*. 2008 Dec;23(10):1269–78.
26. Rooney BD, Derrick TR. Joint contact loading in forefoot and rearfoot strike patterns during running. *J Biomech*. 2013;46(13):2201–6.
27. Crownshield RD, Brand RA, Johnston RC. The effects of walking velocity and age on hip kinematics and kinetics. *Clin Orthop Relat Res*. 1978 May;(132):140–4.
28. Röhrle H, Scholten R, Sigolotto C, Sollbach W, Kellner H. Joint forces in the human pelvis-leg skeleton during walking. *J Biomech*. 1984;17(6):409–24.
29. Speirs AD, Heller MO, Duda GN, Taylor WR. Physiologically based boundary conditions in finite element modelling. *J Biomech*. 2007 Jan;40(10):2318–23.
30. Wagner DW, Divringi K, Ozcan C, Grujicic M, Pandurangan B, Grujicic A. Combined musculoskeletal dynamics/structural finite element analysis of femur physiological loads during walking. *Multidiscipline Model Mater Struct*. 2010;6(4):417–37.
31. Delp SL, Anderson FC, Arnold AS, et al. OpenSim: open-source software to create and analyze dynamic simulations of movement. *IEEE Trans Biomed Eng*. 2007 Nov;54(11):1940–50.
32. Hamner SR, Seth A, Delp SL. Muscle contributions to propulsion and support during running. *J Biomech*. 2010 Oct 19;43(14):2709–16.
33. Yamaguchi GT, Zajac FE. A planar model of the knee joint to characterize the knee extensor mechanism. *J Biomech*. 1989 Jan;22(1):1–10.
34. De Groote F, De Laet T, Jonkers I, De Schutter J. Kalman smoothing improves the estimation of joint kinematics and kinetics in marker-based human gait analysis. *J Biomech*. 2008 Dec 5;41(16):3390–8.
35. Crownshield RD. Use of optimization techniques to predict muscle forces. *J Biomed Eng*. 1978 May 1;100(2):88–92.
36. Murray MP. Gait as a total pattern of movement. *Am J Phys Med*. 1967 Feb;46(1):290–333.
37. Moision KC, Sumner DR, Shott S, Hurwitz DE. Normalization of joint moments during gait: a comparison of two techniques. *J Biomech*. 2003 Apr;36(4):599–603.
38. Field A. *Discovering statistics using IBM SPSS statistics*. London: Sage Publications 2013.
39. Fukuchi RK, Duarte M. Comparison of three-dimensional lower extremity running kinematics of young adult and elderly runners. *J Sports Sci*. 2008 Nov;26(13):1447–54.
40. Pandy MG, Andriacchi TP. Muscle and joint function in human locomotion. *Annu Rev Biomed Eng*. 2010 Aug 15;12:401–33.
41. Geijtenbeek T, Steenbrink F, Otten B, Even-Zohar O. D-flow: immersive virtual reality and real-time feedback for rehabilitation. In: *Proceedings of the 10th International Conference on Virtual Reality Continuum and Its Applications in Industry*. New York: ACM; 2011. p. 201–8. [Presented at VRCAI '11 The 10th International Conference on Virtual Reality Continuum and Its Applications in Industry; Hong Kong, China; 2011 Dec 11–12, 2011]. DOI:10.1145/2087756.2087785 .
42. Prince F, Corriveau H, Hébert R, Winter DA. Gait in the elderly. *Gait Posture*. 1997;5(2):128–35.
43. Kerrigan DC, Franz JR, Keenan GS, Dicharry J, Della Croce U, Wilder RP. The effect of running shoes on lower extremity joint torques. *PM R*. 2009;1(12):1058–63. DOI:10.1016/j.pmrj.2009.09.011 .
44. Keenan GS, Franz JR, Dicharry J, Della Croce U, Kerrigan DC. Lower limb joint kinetics in walking: the role of industry recommended footwear. *Gait Posture*. 2011 Mar;33(3):350–5.